

Theoretical study of the water tetramer

David J. Wales and Tiffany R. Walsh

University Chemical Laboratories, Lensfield Road, Cambridge CB2 1EW, United Kingdom

(Received 18 December 1996; accepted 22 January 1997)

We report rearrangement mechanisms and new stationary points for the water tetramer and deduce the associated tunneling splitting patterns and nuclear spin weights when different processes are assumed to be feasible. The basis sets employed for the *ab initio* calculations are double-zeta plus polarization (DZP) and DZP with additional diffuse functions (DZP+diff), and results have been obtained within both the Hartree–Fock (HF) and density functional theory frameworks employing the Becke exchange and the Lee–Yang–Parr correlation functionals (BLYP). The results are compared with those found for a relatively sophisticated empirical rigid-body intermolecular potential. One direct degenerate rearrangement of the cyclic global minimum was characterized in the HF calculations, but disappears when density functional theory is applied. The latter mechanism involves a larger barrier than pathways mediated by higher index saddle points belonging to the torsional space. In principle, doublet splittings could result from tunneling via a number of possible routes, and further calculations will be needed to elucidate the dynamics for this system. © 1997 American Institute of Physics. [S0021-9606(97)51616-3]

I. INTRODUCTION

Far-infrared vibration-rotation tunneling (FIR-VRT) spectroscopy^{1–4} has recently led to a flurry of experimental and theoretical investigations of small water clusters. For the water, trimer experiment and theory are generally in good agreement. Experiments^{5–8} reveal the facile nature of the single “flip” rearrangement for the cyclic global minimum, which leads to tunneling splittings of order 10 cm^{-1} in $(\text{H}_2\text{O})_3$ and a vibrationally averaged symmetric top spectrum. Much smaller regularly spaced quartet splittings of each line are found at high resolution. To explain such tunneling splittings, theory must characterize the underlying rearrangement mechanisms, and in the present work we focus upon rearrangements of the water tetramer. We will first provide a brief overview of recent results for the water trimer and pentamer, as far as they are relevant to the present study. Further details and references can be found in our recent accounts of rearrangement mechanisms in the water trimer⁹ and pentamer.¹⁰

Pugliano and Saykally⁵ originally suggested three mechanisms to account for the observed tunneling splittings in the trimer. The first of these was the single flip process, previously characterized by Owicki *et al.*¹¹ for an empirical potential. An *ab initio* pathway for this process was subsequently reported by Wales,¹² and the transition state was also found by Fowler and Schaefer.¹³ Wales characterized two other relatively low energy rearrangements for the trimer; the first resembles the “donor tunneling” rearrangement of water dimer¹⁴ and involves a transition state with a bifurcated geometry where one water molecule acts as a double donor and another as a double acceptor. This mechanism is therefore referred to as “donor” or “bifurcation” tunneling. Fowler and Schaefer¹³ also located the corresponding transition state in their study, and in a recent systematic treatment we have found that there are six possible distinct degenerate rearrangements of this type, depending upon the number of

intrinsic flips which accompany the bifurcation.⁹ In each case, the bifurcation mechanism is predicted to produce additional closely spaced quartet splittings.

Further analysis of the trimer spectrum suggested that the bifurcation mechanism is indeed responsible for the quartet splittings.⁶ In the most recent work, further study of the 87.1 cm^{-1} band for $(\text{H}_2\text{O})_3$ has revealed that some of the quartets are further split into doublets, and has provided an assignment for each line.¹⁵ The latter work includes a rigorous derivation of a Hamiltonian for the constrained three-dimensional torsional space of the free hydrogens and provides explicit expressions for the effective moments of inertia and for the Coriolis coupling operator between the internal and overall rotations.¹⁵ The results indicate that the generator for the bifurcation mechanism must contain the inversion operation, and are consistent with our recent systematic study of the bifurcation pathways, which revealed that the three generators associated with only regular quartet splittings all contain the inversion.⁹ Single flip and bifurcation mechanisms have also been reported for the water pentamer.^{10,16}

There have been a number of calculations aimed at further characterization of the dynamics of the water trimer, including the derivation of a rigorous Hamiltonian¹⁷ and calculations of torsional potential energy surfaces and vibrational wave functions.^{18–22} Diffusion Monte Carlo (DMC) calculations have also been performed to calculate vibrationally averaged rotational constants and to estimate tunneling splittings.^{23,24} The DMC approach enables all the intermolecular degrees of freedom to be included, but difficulties arise for the tunneling splitting calculations in finding a suitable empirical potential which reproduces the correct mechanisms and in positioning the nodal surface for the excited vibrational wave functions. Nevertheless, agreement with observed rotational constants is good, and tunneling splittings also seem to be generally reasonable, although direct comparison with experiment is not possible. For the water

pentamer, both DMC calculations²⁴ and a simple perturbation treatment predict observable splittings for the flip which probably lie outside the range scanned experimentally to date.²⁵ The estimated splittings probably agree within the rather large error bounds for these difficult calculations.

The water tetramer is expected to behave rather differently from both the trimer and the pentamer. The global minima of the latter systems have cyclic odd-membered rings, where two neighboring free hydrogen atoms must lie on the same side. These clusters are therefore frustrated, and this is reflected in the existence of a low energy single flip mechanism in each case. For the water tetramer, on the other hand, the cyclic global minimum is not frustrated, and the single flip process does not constitute a degenerate rearrangement. Experimentally,^{26,27} doublet splittings of order 10^{-4} cm⁻¹ have been reported for (D₂O)₄, and the object of the present article is to seek a mechanistic explanation for this observation. Although DMC calculations have revealed a splitting for one empirical potential,²⁴ the interpretation of this result does not seem to be straightforward, as discussed in Sec. IV.

We first discuss the results of geometry optimizations and calculations of rearrangement pathways for two basis sets using both Hartree–Fock and density functional theory approaches. Schütz *et al.*²⁸ have previously reported extensive *ab initio* calculations within the torsional space of the tetramer, including unrestricted geometry optimizations with aug-cc-pVDZP basis sets²⁹ and second order Møller–Plesset (MP2) correlation corrections. Our results are in good agreement with the latter study except for one high lying stationary point. However, we have also found a number of additional stationary points involving bifurcated molecules, including true transition states. We report extensive pathway calculations, harmonic vibrational intensities, counterpoise corrected³⁰ interaction energies, and analyze the effective molecular symmetry groups and tunneling splitting patterns expected when various mechanisms are considered to be feasible. We also compare the *ab initio* results with those obtained for a relatively sophisticated rigid monomer intermolecular potential which should be similar to that employed by Gregory and Clary in their DMC calculations.²⁴ The intermolecular potential does not support the only direct degenerate rearrangement that we have found for the tetramer global minimum; in fact, this mechanism also disappears where density functional theory is used. The topology of the HF potential energy surface (PES) differs systematically from the density functional theory (DFT) and empirical surfaces, as described in the following sections.

II. STATIONARY POINTS FOR THE WATER TETRAMER

Two basis sets were employed in the present *ab initio* calculations, namely double-zeta³¹ plus polarization (DZP), with polarization functions consisting of a single set of *p* orbitals on each hydrogen (exponent 1.0), and a single set of six *d* orbitals on each oxygen (exponent 0.9), and DZP+diff where a diffuse *s* function with exponent 0.0441

is added to each hydrogen atom and diffuse *s* and *p* functions with exponents 0.0823 and 0.0651, respectively, are added to each oxygen atom. Previous work suggests that DFT may be capable of producing results comparable to Hartree–Fock/MP2 calculations^{32,33} when basis sets of similar quality are employed, and may be subject to less basis set superposition error³⁴ (BSSE). There is also evidence³⁵ which suggests that inclusion of diffuse functions in the basis set can help to reduce the BSSE. Geometry optimizations on the counterpoise-corrected surfaces were deemed too computationally expensive,³⁶ and unnecessary for the present purposes. In the present DFT calculations, we used the Becke nonlocal exchange functional³⁷ and the Lee–Yang–Parr correlation functional³⁸ (referred to collectively as BLYP). The CADPAC package³⁹ was used to calculate all the derivatives, and geometry optimization and pathway calculations were performed with our program OPTIM.⁴⁰ Numerical integration of the BLYP functionals was performed on a grid between the CADPAC “MEDIUM” and “HIGH” options containing a maximum of 130 000 points after removal of those with densities below the preset tolerances.

Further details of the geometry optimizations and pathway calculations can be found elsewhere.¹⁰ The optimizations were deemed to be converged when the rms gradient fell below 10^{-6} atomic units,⁴¹ ensuring that the largest “zero” frequencies of the stationary points were generally less than 0.5 cm⁻¹ for the HF optimizations. Since derivatives of the grid weights were not included in the DFT calculations the zero frequencies can be as large as 20 cm⁻¹ for these stationary points for the same convergence limit. It was, in fact, necessary to include the grid weight derivatives and use the CADPAC HIGH accuracy integration grids to characterize the (*uuud*) minimum and the associated (*udup*) transition state in the DZP+diff/BLYP calculations. At this level of theory, the two stationary points are very similar indeed, indicating that (*uuud*) has only marginal stability in this case. We estimate¹⁰ that the errors in the BLYP energies due to the numerical integrations are of order 10^{-5} Hartree (2 cm⁻¹).

We have also studied the tetramer PES for a rigid-monomer intermolecular potential of the anisotropic site potential (ASP) form due to Millot and Stone.⁴² The particular parametrization differs from the original version in the dispersion terms, the induction damping, and the inclusion of charge transfer—precise details of this complex functional form will be omitted here. Our results are for ASP-W2, which includes distributed multipoles⁴³ up to rank 2 to describe the charge distribution. The first order induction energy without iteration was used, since the results obtained for this potential for the water pentamer with and without iteration were very similar,¹⁰ and iterating the induced moments to convergence is quite time consuming. We note that an ASP potential produced the best results for tunneling splittings of the water dimer in previous work.⁴⁴ All the calculations involving the ASP-W2 potential were performed with our program ORIENT3.⁴⁵

Stationary points from the torsional space, i.e., those

TABLE I. Total energies (hartree) of the water tetramer stationary points found in this study with the ASP-W2 intermolecular potential and at various levels of *ab initio* theory. The Hessian index (the number of negative Hessian eigenvalues) is given in square brackets. Blank entries indicate that the corresponding optimization was not attempted.

Minimum	ASP-W2	DZP/HF	DZP+diff/HF	DZP/BLYP	DZP+diff/BLYP
{ <i>udud</i> } <i>S</i> ₄	-0.034 935 8[0]	-304.229 757[0]	-304.239 477[0]	-305.760 10[0]	-305.788 23[0]
{ <i>uudd</i> } <i>C</i> _i	-0.033 733 4[0]	-304.228 238[0]	-304.238 119[0]	-305.757 76[0]	-305.786 28[0]
{ <i>uuuu</i> } <i>C</i> ₂	-0.031 903 1[0]	→{ <i>udud</i> }		-305.754 02[0]	→{ <i>udud</i> }
{ <i>uuud</i> } <i>C</i> ₁	-0.029 815 4[0]	→{ <i>udud</i> }		-305.757 40[0]	-305.786 19[0]
{ <i>udup</i> } <i>C</i> ₁	-0.033 170 7[1]	→{ <i>uudp</i> }		-305.757 18[1]	-305.786 19[1]
{ <i>uupa</i> } <i>C</i> ₁	-0.032 615 1[1]	-304.228 003[1]	-304.237 985[1]	-305.756 28[1]	-305.785 38[1]
{ <i>uudp</i> } <i>C</i> ₁	-0.032 596 3[1]	-304.228 014[1]	-304.237 987[1]	-305.756 30[1]	-305.785 39[1]
{ <i>uuup</i> } <i>C</i> ₁	-0.031 673 1[1]	→{ <i>uudp</i> }		→{ <i>uuud</i> }	
{ <i>updp</i> } <i>C</i> _i	-0.031 726 8[2]	-304.227 870[2]	-304.237 820[2]	-305.755 26[2]	-305.784 68[2]
{ <i>udpp</i> } <i>C</i> ₁	-0.031 614 9[2]	-304.227 959[2]	-304.237 980[2]	→{ <i>udud</i> }	
{ <i>upup</i> } <i>C</i> ₂	-0.031 450 1[2]	→{ <i>upud</i> }		→{ <i>uuud</i> }	
{ <i>uupp</i> } <i>C</i> ₁	-0.030 596 9[2]	→{ <i>updp</i> }		-305.752 91[2]	-305.783 17[2]
{ <i>uppp</i> } <i>C</i> ₁	-0.029 815 4[3]	→{ <i>udpp</i> }		→{ <i>uudp</i> }	
{ <i>pppp</i> } <i>C</i> _{4h}	-0.027 673 3[4]	-304.226 385[4]	-304.236 809[4]	-305.749 22[4]	-305.781 22[4]
{ <i>uubd</i> } <i>C</i> ₁	-0.031 638 8[1]	→{ <i>udbd</i> }		-305.750 56[1]	-305.780 31[1]
{ <i>udbd</i> } <i>C</i> ₁	-0.032 262 6[1]	-304.225 485[1]	-304.235 417[1]	-305.751 89[1]	-305.781 17[1]
{ <i>bpbp</i> } <i>C</i> _{2h}	-0.032 746 3[2]	-304.222 389[2]	-304.232 445[2]	-305.745 94[2]	-305.776 12[2]
{ <i>bbpp</i> } <i>C</i> _s	-0.027 691 7[3]	-304.219 814[3]	-304.229 967[2]	-305.741 58[3]	-305.772 58[3]
{ <i>bbpp</i> } <i>C</i> _s	-0.025 440 8[4]	-304.214 593[3]	-304.224 791[3]	>100 steps	
{ <i>bbbb</i> } <i>S</i> ₄	-0.020 426 4[4]	-304.207 296[4]	-304.217 492[4]	-305.725 08[4]	-305.756 29[4]
{ <i>bbbb</i> } <i>C</i> _{4h}	-0.020 064 6[5]	-304.206 970[5]	-304.217 324[5]	-305.724 19[5]	-305.756 10[5]
<i>ts1 C</i> ₁	-0.031 542 9[1]	>100 steps	-304.229 661[1]	→{ <i>uupd</i> }	→{ <i>uupd</i> }
<i>ts2 C</i> ₁	-0.027 967 7[1]	-304.217 882[1]	-304.229 540[1]	-305.742 36[1]	-305.771 65[1]
<i>ts3 C</i> ₁	-0.032 987 7[1]	>100 steps	>100 steps		
<i>ts4 C</i> ₁	-0.028 613 7[1]	-304.217 395[1]	-304.229 765[1]	-305.741 91[1]	>50 steps
<i>ts5 C</i> ₁	-0.030 842 8[1]	→{ <i>udbd</i> }			
<i>ts6 C</i> ₁	-0.031 818 7[1]	>100 steps			

which can be represented principally in terms of hydrogen atom flips, were constructed following Schütz *et al.*²⁸ Our results agree with the conclusions of the latter authors, in that no true transition state for a direct degenerate rearrangement of the global minimum was found in this set of structures. (A degenerate rearrangement is one in which the two minima differ only by permutations of atoms of the same element.)⁴⁶ Here we adopt Murrell and Laidler's definition of a true transition state as a stationary point with a single negative Hessian eigenvalue.⁴⁷ We therefore searched for further transition states outside the torsional space, particularly in structures containing bifurcated water molecules. The total energies of all the resulting stationary points are summarized in Table I. Here we have used the helpful notation introduced by Schütz *et al.*¹⁸ where the water monomers in a cyclic structure are identified according to whether the free (nonhydrogen bonded) hydrogen is "up," "down," or "planar," which we label *u*, *d*, and *p*, respectively. In the present work, we will identify bifurcated water molecules as "b." The cyclic global minimum may therefore be denoted as (*udud*). The order of the molecules in brackets can be used to distinguish different isomers; the convention is that hydrogen bond donation proceeds from left to right within the brackets. Curly brackets are used to denote the set of permutational isomers based upon a particular structure. All the stationary points are illustrated in Fig. 1.

Properties of selected stationary points including

counterpoise-corrected³⁰ interaction energies, are collected in Table II, and further parameters and vibrational frequencies of the (*udud*) minimum are given in Tables III and Tables IV, for comparison with previous work. The harmonic frequencies of the other stationary points are omitted for brevity.⁴⁰ Xantheas⁴⁹ has recently emphasized the importance of including monomer relaxation in the counterpoise correction, but found that the effect was rather small for the water dimer. We have calculated the counterpoise-corrected interaction energies both with and without monomer relaxation and generally find differences of only around 0.5 mh. The tabulated values include the monomer relaxation.

The first *ab initio* calculations to consider the cyclic tetramer were probably those by Del Bene and Pople⁵⁰ and Lentz and Scheraga.⁵¹ The report of simulations by Briant and Burton⁵² using a pair potential does not include any structural results, but the stability of the cyclic structure was noted by Kistenmacher *et al.*⁵³ in their efforts to develop an intermolecular pair potential based upon *ab initio* calculations. Owicki *et al.*¹¹ found nine local minima for the tetramer with their empirical potential using electrons and nuclei (EPEN) potential, but a tetrahedral structure was found to lie below the (*udud*) minimum. Kim *et al.*⁵⁴ compared the latter results with those obtained from their Matsuoba–Clementi–Yoshimine (MCY) potential and a new parametrization including three- and four-body terms. In this case, the (*udud*) minimum was found to lie lowest, in agreement with

results obtained by Vernon *et al.*⁵⁵ who considered four alternative empirical potentials. Koehler *et al.*⁵⁶ exploited the S_4 symmetry of the $(udud)$ structure to perform geometry optimizations up to the 6-31G**/MP3 level, and analyzed the cooperative nature of the intermolecular forces.

Schröder⁵⁷ employed a reparametrized version of the EPEN potential QPEN/B2, and reported 12 local minima with the $(udud)$ structure lying lowest. Honegger and Leutwyler⁵⁸ performed full geometry optimizations up to the 6-31G*/HF level, with the principal aim of performing normal coordi-

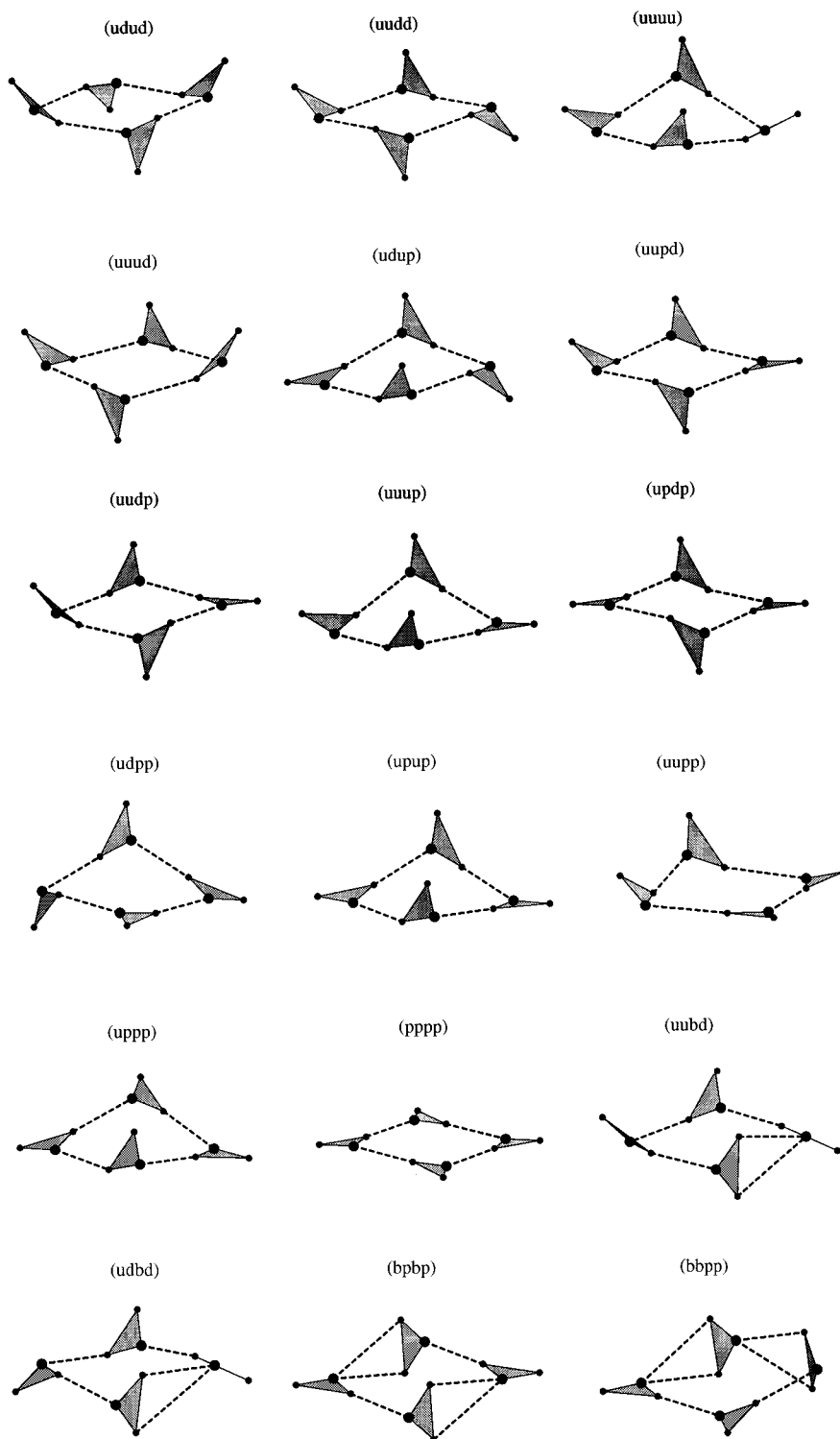


FIG. 1. Stationary points found for the water tetramer in the present work. See also Table I. These graphics were produced using Mathematica (Ref. 48) with the hydrogen bonds specified by a distance cut off. Where the same structure exists at different levels of theory, the geometries are generally indistinguishable by eye. However, the transition states denoted by the label ts changed significantly between reoptimizations; we have chosen to illustrate the ASP-W2 structures in each case.

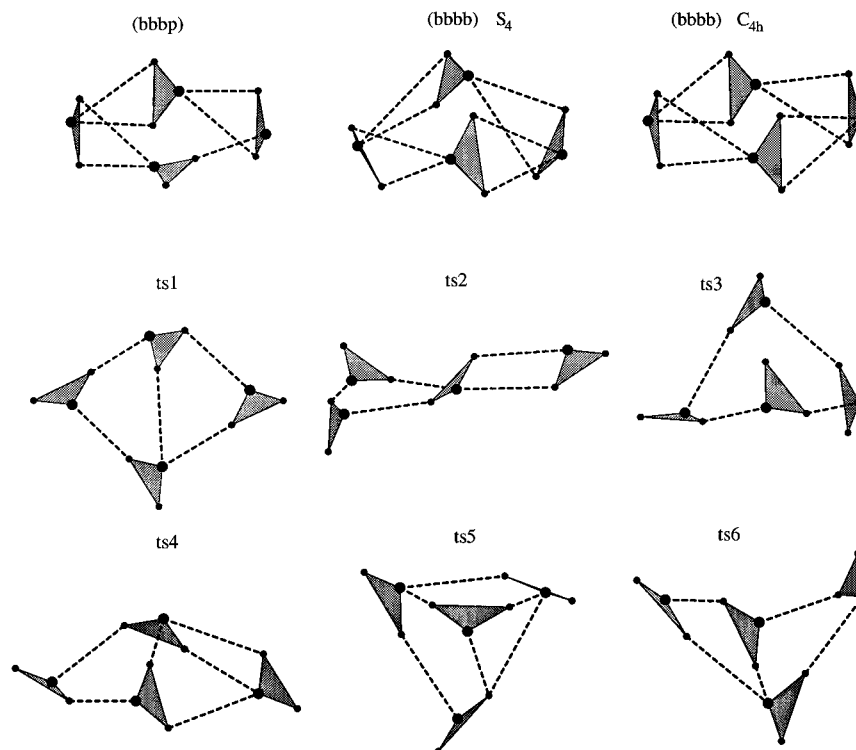


FIG. 1. (Continued.)

nate analysis and studying frequency shifts. They argued that this level of theory should give a reasonably good description of the structure and vibrations. Herndon and Radhakrishnan reached similar conclusions.⁵⁹

A systematic search for the global minimum of the MCY potential by Pillardy *et al.*⁶⁰ succeeded in finding the (*udud*) minimum. Bertagnoli⁶¹ has speculated about the significance of this structure for the behavior of bulk water, while

Tsai and Jordan⁶² have characterized a number of minima and transition states for (H₂O)₄ using TIP3P and TIP4P potentials.⁶³ Xantheas and Dunning⁶⁴ and Xantheas³² have performed full geometry optimizations for the (*udud*) minimum in the aug-cc-pVDZ basis²⁹ using Hartree–Fock and density functional theory, respectively. Our DZP+diff/HF and DZP+diff/BLYP frequencies and infrared absorption intensities are compared with their results in Table IV. The

TABLE II. Counterpoise-corrected binding energies including monomer relaxation (mh) and properties of various water tetramer stationary points calculated at the DZP+diff/HF (DZP+diff/BLYP) levels of theory. μ is the magnitude of the dipole moment in debye. The results for the DZP basis are omitted for brevity.

Minimum	Binding energy		Rotational constants/GHz				μ	
{ <i>udud</i> } <i>S</i> ₄	36.0	(51.1)	3.311	3.311	1.687	(3.674 3.674 1.867)	0.00	(0.00)
{ <i>uudd</i> } <i>C</i> ₁	34.8	(49.5)	3.310	3.271	1.658	(3.666 3.627 1.849)	0.00	(0.00)
{ <i>uuud</i> } <i>C</i> ₁		(49.1)				(3.718 3.582 1.857)		(2.13)
{ <i>uupd</i> } <i>C</i> ₁	34.8	(48.6)	3.333	3.246	1.665	(3.795 3.494 1.841)	0.94	(1.38)
{ <i>uudp</i> } <i>C</i> ₁	34.8	(48.7)	3.339	3.241	1.663	(3.792 3.498 1.840)	0.98	(1.36)
{ <i>updp</i> } <i>C</i> ₁	34.7	(48.2)	3.438	3.149	1.653	(3.943 3.369 1.833)	0.00	(0.00)
{ <i>udpp</i> } <i>C</i> ₁	34.8		3.297	3.282	1.668		0.92	
{ <i>uupp</i> } <i>C</i> ₁		(46.5)				(3.616 3.606 1.819)		(3.30)
{ <i>pppp</i> } <i>C</i> _{4h}	33.4	(45.1)	3.270	3.270	1.635	(3.585 3.585 1.793)	0.00	(0.00)
{ <i>u dbd</i> } <i>C</i> ₁	32.4	(44.4)	3.448	3.081	1.645	(3.611 3.485 1.799)	1.13	(0.91)
{ <i>bbpp</i> } <i>C</i> _{2h}	30.0	(39.4)	3.685	2.846	1.629	(3.630 3.281 1.751)	0.00	(0.00)
{ <i>bbpp</i> } <i>C</i> _s	27.8	(36.3)	3.300	2.922	1.571	(3.536 3.119 1.682)	2.12	(1.95)
{ <i>bbbb</i> } <i>C</i> _s	23.0		3.169	2.745	1.500		1.45	
{ <i>bbbb</i> } <i>S</i> ₄	16.1	(20.8)	2.724	2.724	1.450	(2.829 2.829 1.492)	0.00	(0.00)
{ <i>bbbb</i> } <i>C</i> _{4h}	16.1	(20.5)	2.695	2.695	1.380	(2.803 2.803 1.438)	0.00	(0.00)
<i>ts1</i> <i>C</i> ₁	27.1		4.332	1.861	1.584	(3.796 3.493 1.841)	1.83	(1.37)
<i>ts2</i> <i>C</i> ₁	27.0	(36.4)	4.527	1.790	1.513	(6.875 1.474 1.226)	2.94	(1.02)
<i>ts4</i> <i>C</i> ₁	27.2		4.664	1.713	1.454		3.41	

TABLE III. Comparison of parameters obtained for the (*udud*) global minimum. Distances are in Å and equilibrium rotational constants, *A*, *B*, *C* in GHz. The dipole moment always vanishes due to symmetry. I: present work, DZP+diff/HF; II: present work, DZP+diff/BLYP; III: Ref. 58, 6-31G*/HF; IV: Ref. 56, 6-31G**/HF; V: Ref. 64, aug-cc-pVDZ/HF; VI: Ref. 64, aug-cc-pVDZ/MP2; VII: Ref. 32, aug-cc-pVDZ/BLYP; VIII: Ref. 67, large Gaussian basis with a gradient-corrected exchange-correlation functional; IX: Ref. 65, plane wave basis with a gradient-corrected exchange-correlation functional. The optimized parameters obtained at the aug-cc-pVDZ/MP2 level in Ref. 28 agree with the equivalent calculations in Ref. 64. Ranges of values are reported in Refs. 65 and 67, presumably due to incomplete geometry optimization—the average values are given below.

	I	II	III	IV	V	VI	VII	VIII	IX
O··O	2.857	2.711	2.825	2.831	2.880	2.743	2.743	2.734	2.668
O–H··O	0.955	1.006	0.960	0.955	0.953	0.985	1.000	0.998	
Free O–H	0.944	0.976	0.947		0.944	0.965	0.973	0.971	

(*udud*) global minimum was also located in DFT calculations by Laasonen *et al.*,⁶⁵ Lee *et al.*,⁶⁶ and Estrin *et al.*⁶⁷ The contribution of many-body terms to the bonding in this cluster has been further analyzed by Xantheas.⁶⁸

The most extensive previous *ab initio* survey of the tetramer PES is clearly that of Schütz *et al.*,²⁸ who explored the torsional space of cyclic structures. Within this space, our results are in good agreement with theirs, the only discrep-

ancy arising for the relatively unimportant high energy (*uuuu*) structure. We located a *C*₂ symmetry (*uuuu*) minimum with the ASP-W2 potential, but this structure collapsed when it was used as the starting point for DZP/HF and DZP+diff/BLYP optimizations. Table I indicates that the ASP-W2 surface probably contains more stationary points than any of the *ab initio* surfaces, which seems to be a common observation for empirical potentials. Moreover, the

TABLE IV. Comparison of calculated harmonic frequencies in cm⁻¹ for the cyclic global minimum of (H₂O)₄ with previous *ab initio* results. Intensities in km mole⁻¹ are given in brackets. The present DZP results are omitted for brevity. I: present work, DZP+diff/HF; II: present work, DZP+diff/BLYP; III: Ref. 58, 6-31G*/HF; IV: Ref. 64, aug-cc-pVDZ/HF; V: Ref. 64, aug-cc-pVDZ/MP2; VI: Ref. 32, aug-cc-pVDZ/BLYP; VII: Ref. 67, large Gaussian basis with a gradient-corrected exchange-correlation functional. Note that the quality of the geometry optimization can be assessed to some extent by the accuracy of the degeneracy in the states of *E* symmetry.

I	II	III	IV	V	VI	VII
49(0)	61(0)		44(0)	51(0)	52	50(0)
77(3)	103(3)		67(3)	79(2)	90	89(2)
180(0)	220(0)		162(82)	200(46)	210	221(0)
181(105)	247(58)		169(0)	211(0)	223	231(24)
199(2)	264(11)		187(16)	237(61)	248	254(125)
199(2)	264(11)		187(16)	237(59)	248	255(66)
209(1)	282(3)		198(214)	255(197)	259	266(145)
214(256)	293(272)		198(214)	255(199)	259	268(167)
214(256)	293(272)		199(1)	261(0)	264	272(42)
266(0)	342(0)		243(0)	291(0)	297	284(1)
360(0)	443(0)		340(0)	403(0)	413	422(0)
378(23)	484(19)		357(21)	435(21)	451	462(21)
411(42)	500(50)		385(30)	451(40)	464	465(23)
411(42)	500(50)		385(30)	451(39)	464	466(21)
718(459)	837(240)		660(320)	754(171)	756	756(130)
727(296)	903(200)		684(225)	826(166)	836	856(161)
727(296)	903(200)		684(225)	826(166)	836	859(165)
888(0)	1080(0)		834(0)	996(0)	1005	1043(0)
1768(126)	1589(106)	1856	1763(99)	1637(81)	1583	1615(88)
1774(137)	1608(49)	1856	1769(103)	1653(47)	1601	1630(41)
1798(0)	1608(49)	1856	1769(103)	1653(47)	1601	1632(42)
3963(0)	1648(0)	1873	1789(0)	1683(0)	1632	1660(0)
4008(824)	3083(0)	3855	3936(0)	3391(0)	3111	3124(6)
4008(824)	3210(1857)	3915	3986(756)	3484(1349)	3226	3238(1554)
4029(8)	3210(1857)	3915	3986(756)	3484(1349)	3226	3245(1549)
4237(154)	3260(17)	3943	4004(9)	3522(20)	3269	3286(55)
4238(185)	3748(60)	4143	4203(135)	3886(102)	3723	3720(31)
4238(185)	3748(70)	4143	4204(169)	3887(126)	3724	3721(41)
4239(0)	3748(70)	4143	4204(169)	3887(126)	3724	3723(36)
4239(0)	3749(0)	4144	4205(0)	3887(0)	3724	3725(40)

TABLE V. Rearrangement mechanisms mediated by true transition states in (H₂O)₄. The energies are relative to the (*udud*) global minimum rounded to the nearest cm⁻¹ without zero point corrections. Min₁ is the lower minimum, Δ₁ is the higher barrier, *ts* is the transition state, and Δ₂ is the smaller barrier corresponding to the higher minimum Min₂. *S* is the path length in bohr, *D* is the displacement between minima in bohr, and γ is the cooperativity index. All these quantities are defined in Sec. III.

Min ₁	Δ ₁	<i>ts</i>	Δ ₂	Min ₂	<i>S</i>	<i>D</i>	γ	Description
DZP/HF								
(<i>udud</i>)	382	(<i>uudp</i>)	49	(<i>dduu</i>)	4.8	3.4	3.1	double flip (2a)
(<i>udud</i>)	385	(<i>uupd</i>)	52	(<i>uudd</i>)	5.3	3.4	3.1	double flip (2b)
(<i>udud</i>)	937	(<i>ubbd</i>)	937	(<i>udud</i>)	11.0	4.3	5.1	bifurcation+flip (2c)
DZP+diff/HF								
(<i>udud</i>)	327	(<i>uudp</i>)	29	(<i>uudd</i>)	4.4	3.3	3.1	double flip (2a)
(<i>udud</i>)	327	(<i>uupd</i>)	29	(<i>uudd</i>)	4.9	3.3	3.1	double flip (2b)
(<i>udud</i>)	891	(<i>ubbd</i>)	891	(<i>udud</i>)	10.6	4.3	5.1	bifurcation+flip (2c)
DZP/BLYP								
(<i>udud</i>)	645	(<i>udup</i>)	49	(<i>uduu</i>)	3.3	2.3	5.0	single flip (2d)
(<i>uudd</i>)	320	(<i>uudp</i>)	242	(<i>uudu</i>)	3.9	2.5	4.9	single flip (2e)
(<i>uudd</i>)	325	(<i>uupd</i>)	247	(<i>uuud</i>)	3.8	2.5	4.9	single flip (2f)
(<i>udud</i>)	1806	(<i>ubbd</i>)	1211	(<i>uddd</i>)	11.0	4.3	5.1	bifurcation (2g)
(<i>uudd</i>)	1577	(<i>uubd</i>)	1450	(<i>uuud</i>)	8.2	4.1	5.3	bifurcation (2h)
DZP+diff/BLYP								
(<i>udud</i>)	448	(<i>udup</i>)	0.6	(<i>uduu</i>)	2.3	1.7	5.1	single flip (2d)
(<i>uudd</i>)	195	(<i>uudp</i>)	176	(<i>uudu</i>)	3.9	2.7	4.1	single flip (2e)
(<i>uudd</i>)	200	(<i>uupd</i>)	178	(<i>uuud</i>)	4.0	2.7	4.0	single flip (2f)
(<i>udud</i>)	1545	(<i>ubbd</i>)	1099	(<i>uddd</i>)	10.4	4.3	5.3	bifurcation (2g)
(<i>uudd</i>)	1309	(<i>uubd</i>)	1288	(<i>uuud</i>)	8.8	4.3	4.9	bifurcation (2h)
ASP-W2								
(<i>udud</i>)	387	(<i>udup</i>)	85	(<i>uuud</i>)	4.0	2.6	9.9	single flip (2d)
(<i>uudd</i>)	250	(<i>uudp</i>)	211	(<i>uudu</i>)	4.0	3.0	9.4	single flip (2e)
(<i>uudd</i>)	245	(<i>uupd</i>)	207	(<i>uuud</i>)	4.2	3.0	9.3	single flip (2f)
(<i>udud</i>)	284	(<i>ubbd</i>)	587	(<i>uddd</i>)	7.0	3.8	5.8	bifurcation (2g)
(<i>uudd</i>)	460	(<i>uubd</i>)	421	(<i>uuud</i>)	5.9	4.0	5.7	bifurcation (2h)

(*uuud*) minimum could not be located in our HF calculations, but is supported by the BLYP functional. Most stationary points found in our HF calculations are preserved when the BLYP functional is employed. However, the topology of the potential energy surfaces is different, and this has implications for our interpretation of the observed tunneling splitting, as discussed in following sections. The higher energy transition states bearing the label ‘‘*ts*’’ were first obtained for the ASP-W2 potential and all involve disruption of the cyclic structure. The latter geometries changed significantly between geometry reoptimizations at different levels of theory.

III. TOPOLOGY OF THE POTENTIAL ENERGY SURFACES

Schütz *et al.*²⁸ have previously described the connectivity of their PES within the torsional space in some detail. Our HF surfaces basically agree with theirs within this set of stationary points. However, there is no direct connection between different permutational isomers of the global minimum through a single true transition state in this space. It was this observation, and the discovery of doublet splittings²⁶ in the FIR-VRT spectrum of (D₂O)₄, which prompted us to perform the present study.

We first consider the three pathways corresponding to the true transition states found in both the HF and DFT calculations, and compare these with the results for the

ASP-W2 potential. Since an empirical potential which reproduces the pertinent mechanisms is required for DMC calculations of tunneling splittings,²³ these comparisons are of some interest. Characteristics of the pathways are summarized in Table V, and the mechanisms are illustrated in Fig. 2. Note that the barrier heights are uniformly larger in the BLYP calculations, a feature that we view with suspicion.

Three additional parameters are included in Table V. The first is the integrated path length, *S*, which was calculated as a sum over eigenvector-following steps as in previous work.^{10,12} The second is the distance between the two minima in nuclear configuration space, *D*. The third is the moment ratio of displacement,⁶⁹ γ, which gives a measure of the cooperativity of the rearrangement:

$$\gamma = \frac{N \sum_i [\mathbf{Q}_i(s) - \mathbf{Q}_i(t)]^4}{(\sum_i [\mathbf{Q}_i(s) - \mathbf{Q}_i(t)]^2)^2},$$

where $\mathbf{Q}_i(s)$ is the position vector in Cartesian coordinates for atom *i* in minimum *s*, etc., and *N* is the number of atoms. If every atom undergoes the same displacement in one Cartesian component then γ=1, while if only one atom has one nonzero component then γ=*N*, i.e., 12 for (H₂O)₄. Hence it is clear from Table V that the single flip mechanisms are the most localized and have the shortest paths. The calculated energy profiles corresponding to the five DZP/BLYP pathways described in Table V are shown in Fig. 3.

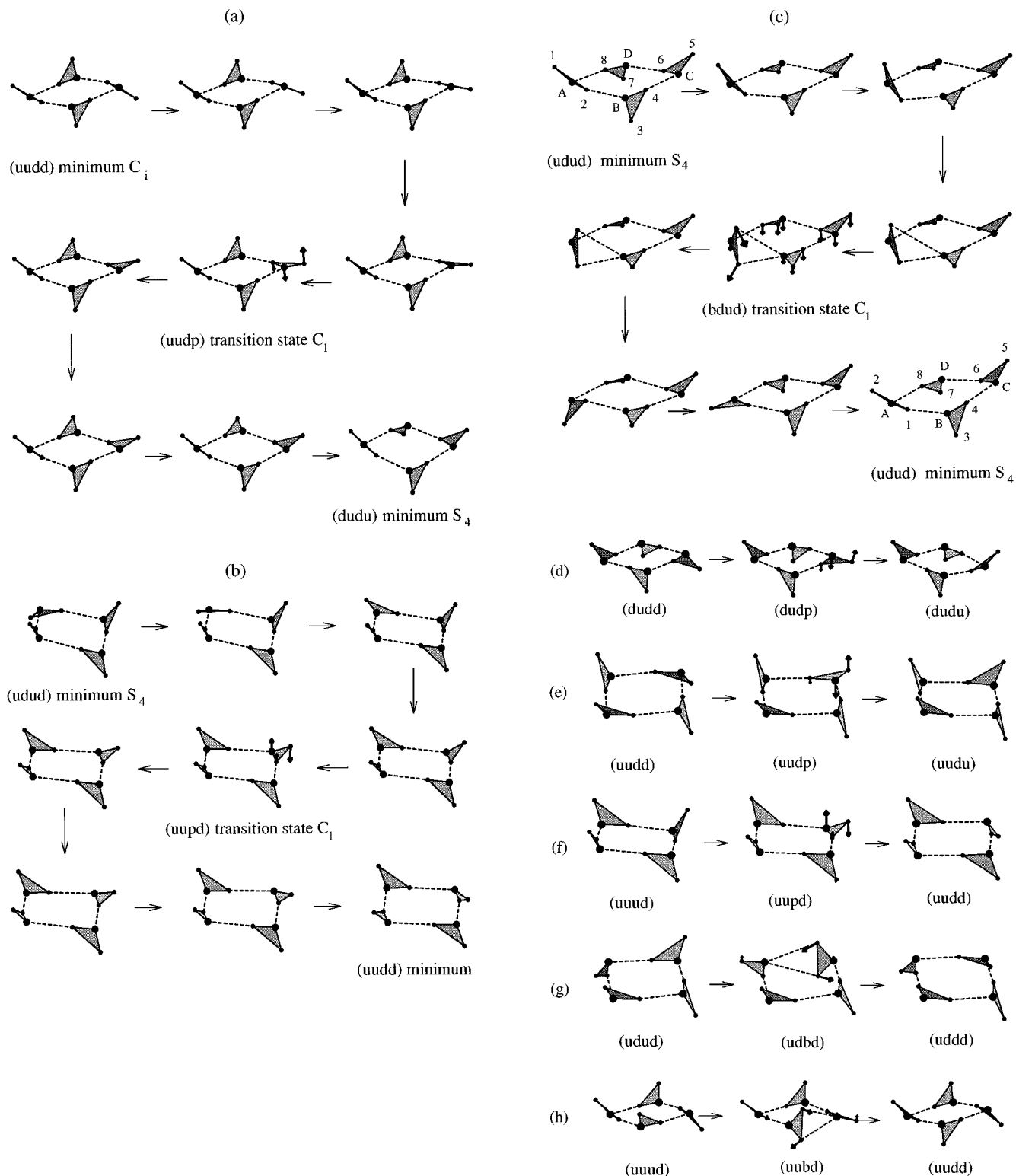


FIG. 2. Rearrangement mechanisms calculated *ab initio* for $(\text{H}_2\text{O})_4$. (a) Asynchronous double flip for the $(uudp)$ transition state (DZP/HF). (b) Asynchronous double flip for the $(uupd)$ transition state (DZP/HF). (c) Degenerate rearrangement of $(udud)$ via a bifurcated $(ubdb)$ transition state (DZP/HF). (d) Single flip for the $(dudp)$ transition state (DZP/BLYP). (e) Single flip for the $(uudp)$ transition state (DZP/BLYP). (f) Single flip for the $(uupd)$ transition state (DZP/BLYP). (g) Bifurcation rearrangement for transition state $(ubdb)$ (DZP/BLYP). (h) Bifurcation rearrangement for transition state $(uubd)$ (DZP/BLYP).

The pathways are represented graphically by three or nine snapshots, depending upon the complexity of the mechanism. The two end points are the two minima and the center structure is the transition state; three other geometries

may be chosen at appropriate points along the two sides of the path to give a better idea of the mechanism. In addition, a suitably scaled transition vector is superimposed on each transition state; this displacement vector is parallel (or anti-

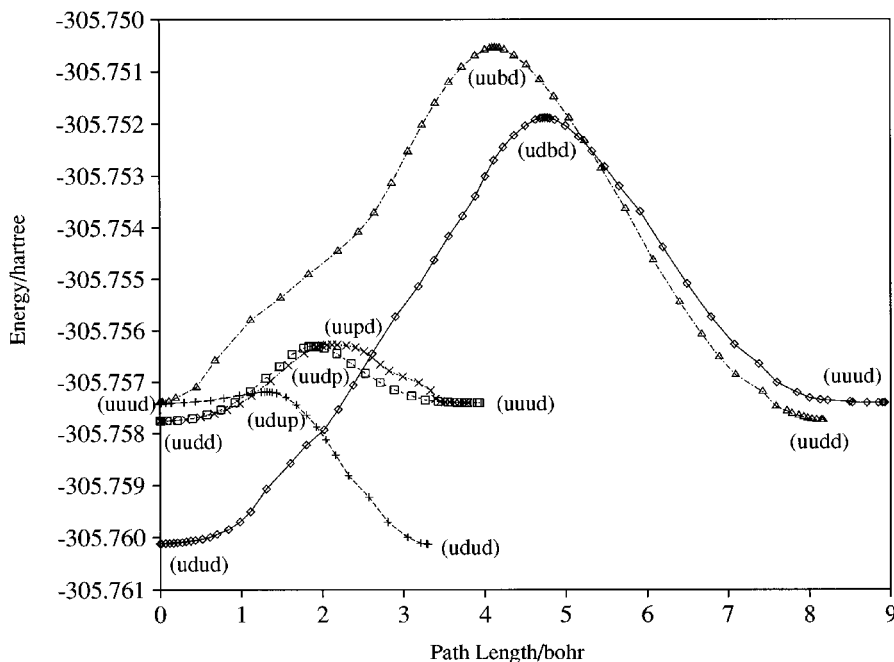


FIG. 3. Calculated energies as a function of the integrated path length, S , for five pathways characterized at the DZP/BLYP level of theory. See also Table V.

parallel) to the (nonmass weighted) Hessian eigenvector corresponding to the unique negative eigenvalue. All of the pathways were calculated by eigenvector—following in nonmass-weighted coordinates; different definitions for reaction pathways have been compared for the water trimer elsewhere.⁹ All our pathways are for the Born–Oppenheimer surface, and do not include any zero-point effects—the barriers corrected for zero-point energies can be obtained from the authors on request.⁴⁰

Table V and Fig. 3 show how the three transition states (*uupd*), (*uudp*), and (*uadb*) mediate different rearrangement mechanisms for the HF and DFT calculations; the topology for ASP-W2 is the same as for the DFT potential energy surfaces for these pathways. The difference is due to the presence of the (*uuud*) structure as a local minimum on the DFT and ASP-W2 surfaces. We did not locate a (*uuud*) stationary point in our HF calculations, and Schütz *et al.*²⁸ were also unable to find it in their study. Hence, when a single flip occurs for (*udud*) on the HF surfaces, the system finds itself in an unfavorable configuration. A second flip on a neighboring molecule is therefore necessary to reach a (*uudd*)-type minimum. Figures 3(a) and 3(b) clearly show how the double flips mediated by the HF (*uupd*) and (*uudp*) transition states actually occur almost one at a time via a single transition state. The two pathways therefore involve highly asynchronous counter rotation of two free hydrogens, not synchronous as suggested by Schütz *et al.*²⁸ Two additional pathways associated with the (*uuud*) minimum were also located in the DFT calculations (see Table V and Fig. 2).

Hence, if we restrict ourselves to the stationary points within the torsional space of cyclic structures, there is no direct link between permutational isomers of the global mini-

um involving a single true transition state. This point was appreciated by Schütz *et al.*,²⁸ who therefore suggested that the tetramer dynamics would be more difficult to explain than the dynamics of the trimer. Previous attempts to rationalize the doublet splittings observed experimentally^{24,26} for (D₂O)₄ therefore appear to invoke either tunneling via the higher index saddle point (*pppp*) or a stepwise process via a (*uudd*) minimum. It is not clear to us how the nodal surface was arranged in previous DMC calculations,²⁴ or what the calculated energy difference in that work corresponds to mechanistically.

It is perhaps worth discussing the topology of the tetramer PES further in the light of the Murrell–Laidler theorem,⁴⁷ which states that if two minima are linked via a higher index saddle point then there must be a path between them of lower energy which involves only true transition states (saddles of index one). This does not mean that the two minima need to be connected via a single transition state, although this is often the case. Hence, even if we restrict our attention to the torsional stationary points, the theorem is not violated, since the two permutational isomers that are linked by the (*pppp*) saddle point can be reached via transition states (*uudp*) and (*uupd*) and the intermediate minimum (*uudd*) (on the HF surfaces). A schematic view of the resulting connectivity is shown in Fig. 4, in which we elaborate upon the octahedral representation suggested by Schütz *et al.*²⁸

As we see from Table V and Fig. 2(c), there is, in fact, a true transition state connecting permutational isomers of the global minimum on the HF potential energy surfaces. However, this direct connection disappears in the DFT calculations and is also absent for ASP-W2. The mechanism can be described as a bifurcation followed by a single flip of the

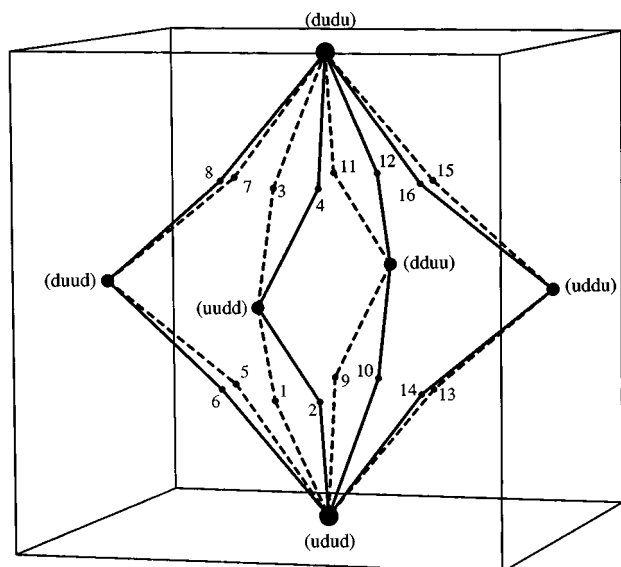


FIG. 4. Schematic view of the rearrangement pathways mediated by permutational isomers of the true transition states ($uudp$) and ($uupd$) which connect two distinct permutational isomers of the global minimum via four permutational isomers of the ($uudd$) minimum. The two different sorts of rearrangement are indicated by solid and broken lines and a consistent ordering has been maintained in our descriptions of the water monomers as u , d , or p .

same monomer, which interchanges the roles of the two hydrogens bound to this molecule. On the HF surface, the initial bifurcation rearrangement leads to a ($uuud$)-type structure, for which there is no corresponding minimum, and a further flip is required, as for the ($uudp$) and ($uupd$) pathways. For the DFT and ASP-W2 potentials, the ($uuud$) structure is a minimum, and so no further rearrangement occurs. The HF ($uabd$) process is an asymmetric degenerate rearrangement, since the two sides of the path are inequivalent.⁷⁰ The implications of all these mechanisms are discussed in Sec. IV.

The ($uabd$) transition state generally lies either above or close to the ($pppp$) and ($udpp$) and ($updp$) saddles in the *ab initio* calculations, and the latter saddles of index two lie below ($pppp$). The other saddle points involving bifurcated molecules are unlikely to play a role in the tunneling dynamics because they are so high in energy. However, if the ($pppp$) saddle is under consideration as a candidate for the tunneling pathway, then for consistency we should also consider the possibility of tunneling via other higher index saddles. Schütz *et al.*²⁸ have illustrated the relative positions of all the stationary points in torsional space, and noted that the ($udpp$) and ($updp$) saddles actually do not lie far above the ($uudp$) and ($uupd$) transition states. Given the choice between tunneling via the ($pppp$) saddle, the index two saddles or the stepwise route involving true transition states it is unclear what the consequences will be for the dynamics. In fact, Schütz *et al.*²⁸ concluded that the ground state should be “well localized within the global minimum.” These uncertainties may also cause problems in defining the nodal surface to calculate the first excited vibrational level by DMC.²⁴

We will only comment briefly on the higher energy path-

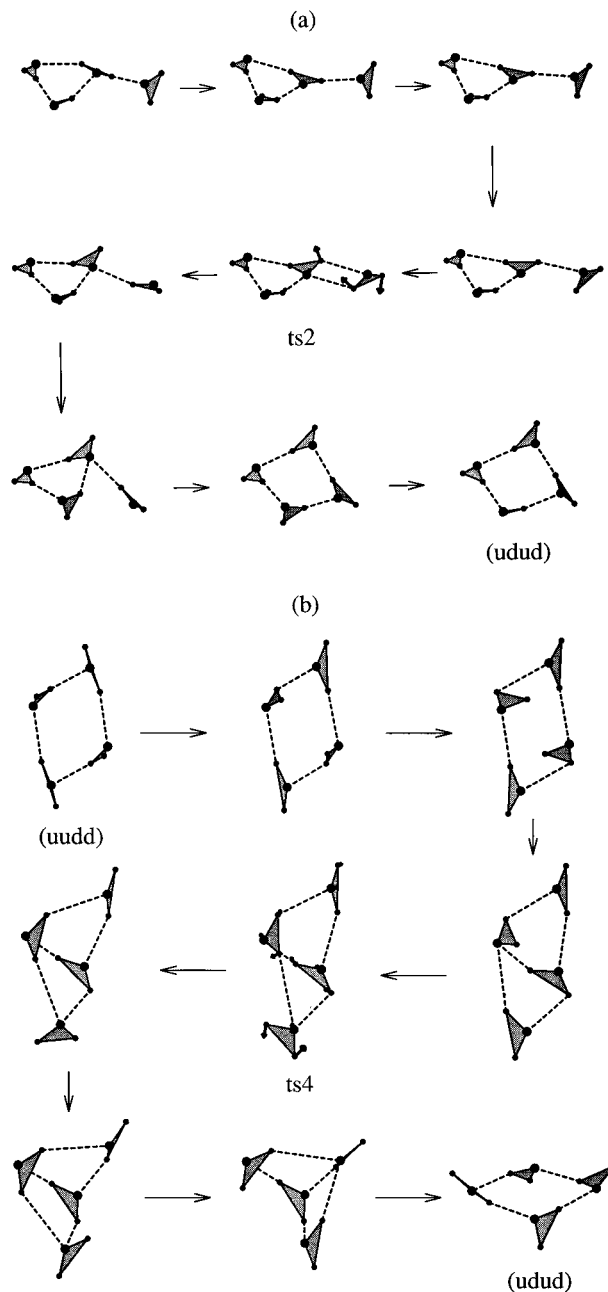


FIG. 5. Pathways for higher energy transition states calculated at the DZP/HF level. (a) Rearrangement from a triangle+terminal minimum (energy $- 304.219\,79\,h$) to the global minimum via $ts2$. (b) Rearrangement from ($uudd$) to ($udud$) via $ts4$. This is a very long and convoluted process.

ways corresponding to transition states labeled “ ts .” We have made no attempt to search exhaustively for such features, and we have only calculated the actual pathways corresponding to these transition states at the DZP/HF level. Here we find that $ts2$ links the ($udud$) minimum to a high energy triangle+terminal minimum, as shown in Fig. 5(a). $ts4$ actually connects the global minimum to a ($uudd$) structure, but does so via a very long and convoluted path which passes through a configuration with a tetrahedral arrangement of water molecules. No *ab initio* stationary points were identified in the present study corresponding to such a tetrahedral structure.

IV. MOLECULAR SYMMETRY GROUPS AND TUNNELING

We now consider the implications of the tunneling pathways discussed above in terms of the effective molecular symmetry group, as in previous studies of the water trimer^{9,12} and pentamer.¹⁰ We will continue to use the notation of Bone *et al.*⁷¹ where a structure specifies a particular geometry which is associated with a number of versions that differ only in the arrangement of labeled atoms of the same element. Tunneling splittings occur when the rovibronic wavefunctions associated with neighboring potential wells interfere with each other, and are generally associated with a low energy degenerate rearrangement mechanism between permutational isomers. Large effects result from low, narrow barriers and small effective masses. An observable effect at the resolution of some given experiment means that the appropriate wave functions are linear combinations of the localized functions from all the different permutational isomers linked by a complete reaction graph corresponding to the mechanism in question. It may be helpful to consider the analogy with the construction of molecular orbitals from linear combinations of atomic orbitals when atoms are brought together within bonding range. The full molecular Hamiltonian is invariant to all permutations of identical nuclei and to inversion of all coordinates through the space fixed origin, and the group of all these operations is called the complete nuclear permutation inversion (CNPI) group. The symmetry adapted linear combinations of localized functions are therefore those which transform according to particular irreducible representations (IR's) of the CNPI group.

The full CNPI group grows in size factorially with the number of equivalent nuclei, and rapidly becomes unwieldy. To alleviate this difficulty, Longuet-Higgins introduced the concept of a "feasible" mechanism,⁷² i.e., one which produces an observable tunneling splitting at the experimental resolution in question. The effective molecular symmetry (MS) group is the subgroup of the CNPI group formed from the permutation inversions (PI's) corresponding to the feasible rearrangements of a given version and a set of PI's which form a group isomorphic to the rigid molecule point group. The MS group has proved to be very useful in classifying the rovibronic energy levels of nonrigid molecules.⁷³ The construction of MS groups, reaction graphs, adjacency matrices, and splitting patterns has been automated using a simple computer program which takes as input a minimal number of generator permutation inversions.^{12,74}

For (H₂O)₄, the CNPI group has dimension $2 \times 4! \times 8! = 1\,935\,360$. However, if we include only PI's in which the same hydrogen atoms are always bound by covalent bonds to the same oxygen atoms, then we define 2520 subgroups of the CNPI group of dimension $2 \times 4! \times (2!)^4 = 768$ each. The set of all feasible rearrangement mechanisms of (H₂O)₄ that do not break covalent bonds must therefore define an MS group which is a subgroup of the group of order 768. Since the (*udud*) global minimum has point group *S*₄, the largest number of versions which could be connected without breaking covalent bonds is $768/4 = 192$. If the gen-

erators corresponding to the feasible rearrangements are known then the splitting pattern for any rovibronic energy level is largely determined by symmetry. However, the magnitude of the splittings depends upon tunneling matrix elements which are generally difficult to calculate for a multi-dimensional tunneling problem. Simple estimates can be obtained rapidly using a perturbation framework, as described elsewhere.⁷⁴ We do not expect these estimates to be accurate to better than a couple of orders of magnitude, but they should still be useful in eliminating some mechanisms from consideration.

As Schütz *et al.*²⁸ have shown, within the torsional space corresponding to a cyclic structure with fixed hydrogen bonds, there are two versions of the (*udud*) minimum, four versions of the (*uudd*) minimum, and eight versions each of the (*uudp*) and (*uupd*) transition states, as shown in Fig. 3. There are also four versions of the (*updp*) and eight versions of the (*udpp*) index two saddles, but only one version of the index 4 (*pppp*) saddle.

If we assume that tunneling occurs between the two versions of (*udud*) in this torsional space, then the effective molecular symmetry group and the splitting pattern do not depend upon the tunneling path. For tunneling via the index 4 (*pppp*) saddle, the (*updp*) or (*udpp*) saddles, or via the transition states (*uupd*) and (*uudp*) with intervening (*uudd*) minima, the molecular symmetry group contains eight elements, as described by Cruzan *et al.*²⁶ who denoted it by *C*_{4h}(*M*) in view of an isomorphism to the *C*_{4h} point group. Furthermore, a doublet splitting pattern would result, in agreement with experiment.²⁶ For each possible path, the same generator PI results if we consider the overall effect of stepwise pathways in terms of a PI applied to the reference version.⁷⁵ Suitable generators for this group include (*ABCD*)(1357)(2468), *E** and (*AC*)(*BD*)(15)(37)(26) × (48)*, where the cycle notation indicates that oxygen *A* is replaced by oxygen *B* etc., and hydrogen 1 by hydrogen 3, etc., for the first generator. *E* denotes the identity permutation and the asterisk indicates inversion of all coordinates through the space-fixed origin. The permutation inversions *E** and (*ABCD*)(1357)(2468) of *C*_{4h}(*M*) correspond to point group operations *i* and *C*₄ of *C*_{4h}. The doublet splitting of the ground state then corresponds to wave functions of *A*_g and *B*_u symmetry at energies of β₁ and -β₁, respectively, where β₁ is the appropriate tunneling matrix element, in agreement with Cruzan *et al.*²⁷

The fact that none of the above paths constitutes a conventional one-step process via a true transition state prompted the present search for further possible mechanisms. The only realistic candidate for an alternative tunneling path is that corresponding to the (*udbd*) transition state, for which a suitable generator is the permutation (12), as we see from Fig. 2(c). This mechanism on its own produces an MS group of order 64, *G*(64), and when combined with a generator for the effective "quadruple flip" a group of order 128, denoted *G*(128), is obtained with a simple direct product structure, as shown in Table VI. The character table for the *G*(64) subgroup is the top left-hand block of the *G*(128) table, and representative operations from each class

TABLE VI. Character table for the group $G(128)$. The number of operations in each class is given and a representative member of each can be found in Table VII.

	1	1	2	4	4	4	4	4	4	8	8	8	8	8	8	1	1	2	4	4	4	4	4	8	8	8	8	8
A_{1g}	1	1	1	1	1	1	1	1	1	1	1	1	1	1	1	1	1	1	1	1	1	1	1	1	1	1	1	1
B_{1g}	1	1	1	1	1	1	1	1	1	-1	-1	-1	-1	-1	-1	1	1	1	1	1	1	1	1	1	-1	-1	-1	-1
A_{2g}	1	1	1	-1	1	-1	1	1	-1	1	-1	-1	1	1	1	1	1	1	-1	1	-1	1	1	-1	-1	-1	-1	1
B_{2g}	1	1	1	-1	1	-1	1	1	-1	-1	1	1	-1	-1	1	1	1	1	-1	1	-1	1	1	-1	-1	1	1	-1
A_{3g}	1	1	1	1	1	1	-1	-1	-1	1	1	-1	-1	1	1	1	1	1	1	1	-1	-1	-1	1	1	-1	-1	-1
B_{3g}	1	1	1	1	1	1	-1	-1	-1	-1	-1	-1	1	1	1	1	1	1	1	1	-1	-1	-1	-1	-1	-1	1	1
A_{4g}	1	1	1	-1	1	-1	-1	-1	1	1	-1	1	-1	1	1	1	1	1	-1	1	-1	-1	-1	1	1	-1	1	-1
B_{4g}	1	1	1	-1	1	-1	-1	-1	1	-1	1	-1	1	1	1	1	1	1	-1	1	-1	-1	-1	1	-1	1	-1	1
E_{1g}	2	2	2	0	-2	0	2	-2	0	0	0	0	0	0	2	2	2	0	-2	0	2	-2	0	0	0	0	0	0
E_{2g}	2	2	2	0	-2	0	-2	2	0	0	0	0	0	0	2	2	2	0	-2	0	-2	2	0	0	0	0	0	0
G_{1g}	4	-4	0	2	0	-2	0	0	0	0	0	0	0	0	4	-4	0	2	0	-2	0	0	0	0	0	0	0	0
G_{2g}	4	-4	0	-2	0	2	0	0	0	0	0	0	0	0	4	-4	0	-2	0	2	0	0	0	0	0	0	0	0
G_{3g}	4	4	-4	0	0	0	0	0	0	0	0	0	0	0	4	4	-4	0	0	0	0	0	0	0	0	0	0	0
A_{1u}	1	1	1	1	1	1	1	1	1	1	1	1	1	1	-1	-1	-1	-1	-1	-1	-1	-1	-1	-1	-1	-1	-1	-1
B_{1u}	1	1	1	1	1	1	1	1	1	-1	-1	-1	-1	-1	-1	-1	-1	-1	-1	-1	-1	-1	-1	-1	-1	-1	-1	-1
A_{2u}	1	1	1	-1	1	-1	1	1	-1	1	-1	-1	1	-1	-1	-1	-1	1	-1	1	-1	1	-1	-1	1	1	-1	-1
B_{2u}	1	1	1	-1	1	-1	1	1	-1	-1	1	1	-1	-1	-1	-1	-1	1	-1	1	-1	-1	-1	1	1	-1	-1	1
A_{3u}	1	1	1	1	1	1	-1	-1	-1	1	1	-1	-1	-1	-1	-1	-1	-1	-1	-1	-1	-1	1	1	1	-1	-1	1
B_{3u}	1	1	1	1	1	1	-1	-1	-1	-1	-1	-1	1	1	-1	-1	-1	-1	-1	-1	-1	-1	1	1	1	1	-1	-1
A_{4u}	1	1	1	-1	1	-1	-1	-1	1	1	-1	-1	1	-1	-1	-1	-1	1	-1	1	-1	1	1	1	-1	-1	1	-1
B_{4u}	1	1	1	-1	1	-1	-1	-1	1	-1	1	-1	1	-1	-1	-1	-1	1	-1	1	-1	1	1	1	-1	-1	1	-1
E_{1u}	2	2	2	0	-2	0	2	-2	0	0	0	0	0	0	-2	-2	-2	0	2	0	-2	2	0	0	0	0	0	0
E_{2u}	2	2	2	0	-2	0	-2	2	0	0	0	0	0	0	-2	-2	-2	0	2	0	2	-2	0	0	0	0	0	0
G_{1u}	4	-4	0	2	0	-2	0	0	0	0	0	0	0	0	-4	4	0	-2	0	2	0	0	0	0	0	0	0	0
G_{2u}	4	-4	0	-2	0	2	0	0	0	0	0	0	0	0	-4	4	0	2	0	-2	0	0	0	0	0	0	0	0
G_{3u}	4	4	-4	0	0	0	0	0	0	0	0	0	0	0	-4	-4	4	0	0	0	0	0	0	0	0	0	0	0

are given in Table VII. The nuclear spin weights for (H₂O)₄ and (D₂O)₄ in $C_{4h}(M)$, $G(64)$, and $G(128)$ are given in Tables 8, 9, and 10, respectively.

For the (*udbd*) bifurcation+flip mechanism alone, each version of the (*udud*) minimum is adjacent to four other permutational isomers and each set of 192 versions of this structure which can be obtained without breaking chemical bonds

is partitioned into 12 domains⁷⁶ containing 16 versions each. The splitting pattern is

$$4\beta_2(A_1), \quad 2\beta_2(G_1), \quad 0(G_3 \oplus E_2), \\ -2\beta_2(G_2), \quad -4\beta_2(A_2),$$

where we have omitted the *g/u* labels which are irrelevant for $G(64)$ and β_2 is the appropriate tunneling matrix element. The accidental degeneracy is typical of Hückel calculations,⁷⁷ and the largest splittings of $\pm 4\beta_2$ simply reflect the connectivity of the reaction graph. Since every energy level λ has a partner with energy $-\lambda$ we can also deduce that the reaction graph contains no odd-membered rings.⁷⁸ Since the dipole moment operator transforms as B_1 in $G(64)$ the selection rule for allowed transitions between nondegenerate states is $A_n \leftrightarrow B_n$. However, B_1 is contained

TABLE VII. Representative permutation-inversion operations for classes 1–13 of the group $G(128)$ [and $G(64)$] in the same order as in Table II. Cycle notation is used, so that $(ABCD)(1357)(2468)$ means that oxygen *A* is replaced by *B*, *B* by *C* etc., hydrogen 1 by hydrogen 3, 3 by 5 and so forth. Cycles of unit length are omitted for clarity. The operations in classes 14–26 of $G(128)$ are the same as those in 1–13, respectively, with an additional factor of E^* .

Class	Operations	Representative PI
1	1	E
2	1	(12)(34)(56)(78)
3	2	(12)(56)
4	4	(12)
5	4	(12)(34)
6	4	(12)(34)(56)
7	4	(AC)(BD)(1526)(3748)
8	4	(AC)(BD)(15)(26)(37)(48)
9	8	(AC)(BD)(1526)(37)(48)
10	8	(ABCD)(13682457)*
11	8	(ABCD)(1357)(2468)*
12	8	(ADCB)(17642853)*
13	8	(ADCB)(1753)(2864)*

TABLE VIII. Absolute nuclear spin weights calculated for the molecular symmetry group $C_{4h}(M)$ for (H₂O)₄ and (D₂O)₄. Tunneling levels have been labeled to coincide with the notation of Cruzan *et al.* (Ref. 27) except that we use \pm subscripts to distinguish the two components of the E IRs to avoid confusion with the E_1 and E_2 IRs of $G(64)$ and $G(128)$.

Irreducible representations	(H ₂ O) ₄	(D ₂ O) ₄
A_g, A_u	70	1665
B_g, B_u	66	1656
$E_g^+, E_g^-, E_u^+, E_u^-$	60	1620

TABLE IX. Absolute nuclear spin weights calculated for the molecular symmetry group $G(64)$ for (H₂O)₄ and (D₂O)₄.

Irreducible representations	(H ₂ O) ₄	(D ₂ O) ₄
A_1, B_1	1	666
A_2, B_2	45	45
A_3, B_3	0	630
A_4, B_4	36	36
E_1	6	306
E_2	12	342
G_1	6	1296
G_2	54	324
G_3	18	348

in the direct products of all the degenerate IR's in $G(64)$, and so doublet splittings are not expected in this case.

If both the bifurcation+flip and effective quadruple flip mechanisms are feasible, then the MS group is $G(128)$ whose character table is given in Table VII. Each set of 192 versions of the (*udud*) structure which can be obtained without breaking chemical bonds is then partitioned into 6 domains⁷⁶ containing 32 versions each. The ground state splitting pattern is then

$$\begin{aligned}
 &4\beta_2 + \beta_1(A_{1g}), \quad 2\beta_2 + \beta_1(G_{1g}), \quad \beta_1(G_{3g} \oplus E_{2g}), \\
 &-2\beta_2 + \beta_1(G_{2g}), \quad -4\beta_2 + \beta_1(A_{2g}), \\
 &4\beta_2 - \beta_1(A_{1u}), \quad 2\beta_2 - \beta_1(G_{1u}), \quad -\beta_1(G_{3u} \oplus E_{2u}), \\
 &-2\beta_2 - \beta_1(G_{2u}), \quad -4\beta_2 - \beta_1(A_{2u}).
 \end{aligned}$$

The dipole moment operator transforms like B_{1u} in $G(128)$ and so doublet splittings would not be expected.

We have estimated the magnitude of the tunneling matrix element β for the possible pathways using the simple perturbation theory described elsewhere.⁷⁴ We emphasize that these estimates are only expected to be accurate to an order of magnitude at best, but may be helpful in comparing the merits of the different paths. We have employed the following assumptions in these estimates. First, we take the barrier heights to be the DZP+diff/HF energy differences

TABLE X. Absolute nuclear spin weights calculated for $G(128)$ when both the effective quadruple flip and (*ubd*) bifurcation+flip mechanism are feasible, for (H₂O)₄ and (D₂O)₄.

Irreducible representations	(H ₂ O) ₄	(D ₂ O) ₄
A_{1g}, B_{1u}	1	336
B_{1g}, A_{1u}	0	330
A_{2g}, B_{2u}	21	21
B_{2g}, A_{2u}	24	24
$A_{3g}, B_{3g}, A_{3u}, B_{3u}$	0	315
$A_{4g}, B_{4g}, A_{4u}, B_{4u}$	18	18
E_{1g}, E_{1u}	3	153
E_{2g}, E_{2u}	6	171
G_{1g}, G_{1u}	3	648
G_{2g}, G_{2u}	27	162
G_{3g}, G_{3u}	9	324

between the global minimum and the highest energy stationary point on the path. The path length is assumed to be the same for the paths mediated by (*pppp*), (*updp*), and (*uupd*)/(*uudp*) via (*uudd*), and equal to roughly $6a_0$. For the effective mass, we assume that the system can be separated into two parts, i.e., the moving hydrogen (or deuterium) atoms and the rest, and employ the formula $m_1 m_2 / (m_1 + m_2)$. Considering the largest number of H/D atoms moving at any one time along the pathway, we take m_1 to be the mass of 4, 2, and 1 (H/D) atoms for (*pppp*), (*updp*), and (*ubd*), and (*uupd*)/(*uudp*), respectively. The path length for the (*ubd*) mechanism is taken to be the distance between the (*udud*) isomers in nuclear configuration space for this path, i.e., $4.3a_0$.

The predicted splittings increase in the order (*pppp*) < (*updp*) < (*uupd*)/(*uudp*) for the stationary points in the torsional space because the mechanism becomes more asynchronous in this direction, leading to smaller barriers and smaller reduced masses (by assumption). The estimated magnitudes of β in wave numbers for (H₂O)₄/(D₂O)₄ are then $5 \times 10^{-8}/6 \times 10^{-11}$, $3 \times 10^{-4}/3 \times 10^{-6}$, $10^{-2}/6 \times 10^{-4}$, and $2 \times 10^{-4}/10^{-6}$ for the (*pppp*), (*updp*), (*uupd*)/(*uudp*), and (*ubd*) paths, respectively. The agreement of our estimate for the (*uupd*)/(*uudp*) pathway for (D₂O)₄ with experiment is fortuitous; it is more significant that the latter pathway gives estimated splittings that are significantly larger than for the other mechanisms. The direct route through the index four (*pppp*) saddle has a high barrier and all the hydrogens must move together, which we have assumed to result in a large reduced mass. The (*ubd*) path has an even higher barrier, but a significantly shorter path and presumably a smaller reduced mass because only two hydrogens need to exchange places.

The above considerations are all based on the topology observed in the HF calculations. For the ASP-W2 potential and for the BLYP exchange-correlation functional, the presence of (*uuud*)-type minima would entail more steps in pathways involving either the true transition states or the index 2 saddles. For example, if only true transition states are involved, then the four hydrogen flips occur sequentially, as for the HF pathways, but there would be three intervening minima, i.e., two of type (*uuud*) and one of type (*uudd*). Our assumptions in the previous paragraph would lead us to assign the same path lengths and reduced masses to such pathways, leading us to the same conclusion that the pathway mediated by true transition states seems likely to contribute most to tunneling. Although these paths may look somewhat convoluted, we note that the observed splitting for (D₂O)₄ is small,²⁶ and so a facile, low-barrier mechanism should perhaps not be expected.

V. CONCLUSIONS

We have optimized geometries and calculated rearrangement pathways for the water tetramer with DZP and DZP+diff basis sets using both Hartree-Fock and density functional theory with the BLYP exchange-correlation functional. We have also compared these results with those ob-

tained from the ASP-W2 rigid-monomer intermolecular potential, which generally reproduces the connectivity of the DFT potential energy surface quite well. However, the HF and DFT surfaces are somewhat different because (*uuud*)-type structures are minima in the DFT calculations, but do not appear to correspond to stationary points at the HF level.

The stationary points we have characterized within the restricted torsional space are in good agreement with the previous results of Schutz *et al.*²⁸ However, we find a number of new stationary points involving bifurcated molecules, including one true transition state at a relatively low energy. Moreover, this transition state actually mediates a direct degenerate rearrangement of the (*udud*) global minimum on the HF potential surfaces. The latter rearrangement on its own produces an effective molecular symmetry group of order 64, rather than the $C_{4h}(M)$ group obtained for a synchronous or asynchronous quadruple flip. The latter process could occur via the index 4 (*pppp*) saddle, asynchronous flips, and index 2 saddles or true transition states and higher lying local minima. The details of these asynchronous paths vary between the HF and DFT surfaces: where (*uuud*) structures are encountered on the DFT surface they are minima, but in HF calculations we find that rearrangement pathways escape from such regions via an additional flip. Because the same two permutational isomers are linked by these different routes in the torsional space, the effective molecular symmetry group is $C_{4h}(M)$ in each case, leading to doublet tunneling splittings, as observed experimentally.²⁶ If we assume that the distance between the two minima is the same for each path, since each route produces an effective quadruple flip, then we might expect tunneling via the true transition states (*uudp*) and (*uupd*) to be most important: such routes involve lower barriers and fewer hydrogen atoms in motion at any one time, which may give a smaller reduced mass. However, these possibilities cannot be distinguished by the present calculations, and indeed all of them might contribute.

The direct degenerate rearrangement via a (*ubbd*) transition state has a higher barrier but a shorter path length because only the two hydrogens on a single monomer are exchanged. Simple estimates of the resultant tunneling splittings suggest that the (*ubbd*) route might contribute to the same order as index 2 saddles, although the splitting pattern does not appear to be consistent with experiment. Our estimated splittings should only be taken as suggestive, and quantum mechanical calculations of the nuclear dynamics in at least four dimensions will be needed to provide further insight. Including the possibility of bifurcation as well as flipping is unlikely to be possible, except via diffusion Monte Carlo calculations.²⁴ Unfortunately, the nodal pattern is required as input in the latter procedure to treat the first excited state, but in the present system it is not clear what that pattern should be. Of course, the tunneling splitting might also be sensitive to vibrational excitation, and since experiment can only measure energy differences involving such transitions, it is possible that the ground state might not exhibit any splittings at all. There are no zero spin weights in any of the tunneling levels we have identified for (D₂O)₄.

Finally, we note that the appearance of observable tun-

neling splittings in water clusters via nondegenerate local minima and multistep pathways is not without precedent. Sabo *et al.*⁷⁹ have identified such splittings in their recent calculations on the torsional levels of isotopically mixed water trimers, where the presence of H and D atoms lowers the symmetry and splits the degeneracies observed for (H₂O)₃ and (D₂O)₃.

ACKNOWLEDGMENTS

D.J.W. gratefully acknowledges financial support from the Royal Society of London, assistance from Mr. A. M. Lee with the CADPAC integration grids, and helpful discussions with Professor R. J. Saykally, Dr. A. J. Stone, and Dr. J. K. Gregory. T.R.W. gratefully acknowledges financial support from the Cambridge Commonwealth Trust.

- ¹R. C. Cohen and R. J. Saykally, *J. Phys. Chem.* **94**, 7991 (1990).
- ²N. Pugliano and R. J. Saykally, *J. Chem. Phys.* **96**, 1832 (1992).
- ³R. J. Saykally and G. A. Blake, *Science* **259**, 1570 (1993).
- ⁴K. Liu, J. D. Cruzan, and R. J. Saykally, *Science* **271**, 929 (1996).
- ⁵N. Pugliano and R. J. Saykally, *Science* **257**, 1937 (1992).
- ⁶K. Liu, J. G. Loeser, M. J. Elrod, B. C. Host, J. A. Rzepiela, N. Pugliano, and R. J. Saykally, *J. Am. Chem. Soc.* **116**, 3507 (1994).
- ⁷K. Liu, M. J. Elrod, J. G. Loeser, J. D. Cruzan, M. Brown, and R. J. Saykally, *Faraday Discuss. Chem. Soc.* **97**, 35 (1994).
- ⁸S. Suzuki and G. A. Blake, *Chem. Phys. Lett.* **229**, 499 (1994).
- ⁹D. J. Wales and T. R. Walsh, *J. Chem. Soc. Faraday Trans.* **92**, 2505 (1996).
- ¹⁰D. J. Wales and T. R. Walsh, *J. Chem. Phys.* **105**, 6957 (1996).
- ¹¹J. C. Owicki, L. L. Shipman, and H. A. Scheraga, *J. Phys. Chem.* **79**, 1794 (1975).
- ¹²D. J. Wales, *J. Am. Chem. Soc.* **115**, 11 180 (1993).
- ¹³J. E. Fowler and H. F. Schaefer, *J. Am. Chem. Soc.* **117**, 446 (1995).
- ¹⁴B. J. Smith, D. J. Swanton, J. A. Pople, H. F. Schaefer, and L. Radom, *J. Chem. Phys.* **92**, 1240 (1990).
- ¹⁵A. van der Avoird, E. H. T. Olthof, and P. E. S. Wormer, *J. Chem. Phys.* **105**, 8034 (1996); E. H. T. Olthof, A. van der Avoird, P. E. S. Wormer, K. Liu, and R. J. Saykally, *J. Chem. Phys.* **105**, 8051 (1996).
- ¹⁶D. J. Wales, *Science* **271**, 925 (1996).
- ¹⁷S. S. Xantheas and B. T. Sutcliffe, *J. Chem. Phys.* **103**, 8022 (1995).
- ¹⁸M. Schütz, T. Bürgi, S. Leutwyler, and H. B. Bürgi, *J. Chem. Phys.* **99**, 5228 (1993).
- ¹⁹W. Klopper and M. Schütz, *Chem. Phys. Lett.* **237**, 536 (1995).
- ²⁰J. G. C. M. Van Duijneveldt-van de Rijdt and F. B. Van Duijneveldt, *Chem. Phys. Lett.* **237**, 560 (1995).
- ²¹T. Bürgi, S. Graf, S. Leutwyler, and W. Klopper, *J. Chem. Phys.* **103**, 1077 (1995).
- ²²W. Klopper, M. Schütz, H. P. Lüthi, and S. Leutwyler, *J. Chem. Phys.* **103**, 1085 (1995).
- ²³J. K. Gregory and D. C. Clary, *J. Chem. Phys.* **102**, 7817 (1995); J. K. Gregory and D. C. Clary, *J. Chem. Phys.* **103**, 8924 (1995); J. K. Gregory and D. C. Clary, *J. Phys. Chem.* **100**, 18014 (1996).
- ²⁴J. K. Gregory and D. C. Clary, *J. Chem. Phys.* **105**, 6626 (1996).
- ²⁵K. Liu, M. G. Brown, J. D. Cruzan, and R. J. Saykally, *Science* **271**, 62 (1996).
- ²⁶J. D. Cruzan, L. B. Braly, K. Liu, M. G. Brown, J. G. Loeser, and R. J. Saykally, *Science* **271**, 59 (1996).
- ²⁷J. D. Cruzan, M. G. Brown, K. Liu, L. B. Braly, and R. J. Saykally, *J. Chem. Phys.* **105**, 6634 (1996).
- ²⁸M. Schütz, W. Klopper, H.-P. Lüthi, and S. Leutwyler, *J. Chem. Phys.* **103**, 6114 (1995).
- ²⁹T. H. Dunning, *J. Chem. Phys.* **90**, 1007 (1992); R. A. Kendall, T. H. Dunning, and R. J. Harrison, *J. Chem. Phys.* **96**, 6796 (1992).
- ³⁰S. F. Boys and F. Bernardi, *Mol. Phys.* **19**, 553 (1970).
- ³¹T. H. Dunning, *J. Chem. Phys.* **53**, 2823 (1970).
- ³²S. S. Xantheas, *J. Chem. Phys.* **102**, 4505 (1995).
- ³³C. Lee, H. Chen, and G. Fitzgerald, *J. Chem. Phys.* **102**, 1267 (1995).

- ³⁴J. H. Van Lenthe, J. G. C. M. van Duijneveldt-van de Rijdt, and F. B. van Duijneveldt, *Adv. Chem. Phys.* **69**, 521 (1987).
- ³⁵D. Feller, *J. Chem. Phys.* **96**, 6104 (1992).
- ³⁶F. B. van Duijneveldt, J. G. C. M. van Duijneveldt-van de Rijdt, and J. H. van Lenthe, *Chem. Rev.* **94**, 1873 (1994).
- ³⁷A. D. Becke, *Phys. Rev. A* **38**, 3098 (1988).
- ³⁸C. Lee, W. Yang, and R. G. Parr, *Phys. Rev. B* **37**, 785 (1988).
- ³⁹R. D. Amos and J. E. Rice, *CADPAC: the Cambridge Analytic Derivatives Package*, Issue 4.0; Cambridge: 1987 (unpublished).
- ⁴⁰The programs ORIENT3 and OPTIM, the MS group analysis programs and any further details of all the calculations reported in this article can be obtained from the authors. Please send email requests to dw34@cus.cam.ac.uk or see <http://brian.ch.cam.ac.uk>
- ⁴¹The atomic units of energy and length are the Hartree and Bohr radius, a_0 , where $1h = 4.359\,748 \times 10^{-18}$ J and $a_0 = 5.291\,772 \times 10^{-11}$ m.
- ⁴²C. Millot and A. J. Stone, *Mol. Phys.* **77**, 439 (1992).
- ⁴³A. J. Stone, *Chem. Phys. Lett.* **83**, 233 (1981); A. J. Stone and M. Alderton, *Mol. Phys.* **56**, 1047 (1985).
- ⁴⁴S. C. Althorpe and D. C. Clary, *J. Chem. Phys.* **101**, 3603 (1994); S. C. Althorpe and D. C. Clary, *J. Chem. Phys.* **102**, 4390 (1995).
- ⁴⁵P. L. A. Popelier, A. J. Stone, and D. J. Wales, *J. Chem. Soc. Faraday Discuss.* **97**, 243 (1994); D. J. Wales, P. L. A. Popelier, and A. J. Stone, *J. Chem. Phys.* **102**, 5556 (1995); D. J. Wales, A. J. Stone, and P. L. A. Popelier, *Chem. Phys. Lett.* **240**, 89 (1995).
- ⁴⁶R. E. Leone and P. V. R. Schleyer, *Angew. Chem. Int. Ed. Engl.* **9**, 860 (1970).
- ⁴⁷J. N. Murrell and K. J. Laidler, *J. Chem. Soc. Faraday II* **64**, 371 (1968).
- ⁴⁸Mathematica 2.0 © Wolfram Research Incorporated; S. Wolfram, *Mathematica*, 2nd ed. (Addison-Wesley, Redwood City, 1991).
- ⁴⁹S. S. Xantheas, *J. Chem. Phys.* **104**, 8821 (1996).
- ⁵⁰J. Del Bene and J. A. Pople, *J. Chem. Phys.* **52**, 4858 (1970).
- ⁵¹B. R. Lentz and H. A. Scheraga, *J. Chem. Phys.* **58**, 5296 (1973).
- ⁵²C. L. Briant and J. J. Burton, *J. Chem. Phys.* **63**, 3327 (1975).
- ⁵³H. Kistenmacher, G. C. Lie, H. Popkie, and E. Clementi, *J. Chem. Phys.* **61**, 546 (1974).
- ⁵⁴K. S. Kim, M. Dupuis, G. C. Lie, and E. Clementi, *Chem. Phys. Lett.* **131**, 451 (1986).
- ⁵⁵M. F. Vernon, D. J. Krajnovich, H. S. Kwak, J. M. Lisy, Y. R. Shen, and Y. T. Lee, *J. Chem. Phys.* **77**, 47 (1982).
- ⁵⁶J. E. H. Koehler, W. Saenger, and B. Lesyng, *J. Comput. Chem.* **8**, 1090 (1987).
- ⁵⁷K. P. Schröder, *Chem. Phys.* **123**, 91 (1988).
- ⁵⁸E. Honegger and S. Leutwyler, *J. Chem. Phys.* **88**, 2582 (1988).
- ⁵⁹W. C. Herndon and T. P. Radhakrishnan, *Chem. Phys. Lett.* **148**, 492 (1988).
- ⁶⁰J. Pillardy, K. A. Olszewski, and L. Piela, *J. Mol. Struct.* **270**, 277 (1992).
- ⁶¹C. J. Tsai and K. D. Jordan, *J. Phys. Chem.* **97**, 11227 (1993).
- ⁶²H. Bertagnolli, *Angew. Chem. Int. Ed. Engl.* **31**, 1577 (1992).
- ⁶³W. L. Jorgensen, *J. Am. Chem. Soc.* **103**, 335 (1981); W. L. Jorgensen, *J. Chem. Phys.* **77**, 4156 (1982); W. L. Jorgensen, J. Chandrasekhar, J. D. Madura, R. W. Impey, and M. L. Klein, *J. Chem. Phys.* **79**, 926 (1983).
- ⁶⁴S. S. Xantheas and T. H. Dunning, *J. Chem. Phys.* **99**, 8774 (1993).
- ⁶⁵K. Laasonen, M. Parrinello, R. Car, C. Lee, and D. Vanderbilt, *Chem. Phys. Lett.* **207**, 208 (1993).
- ⁶⁶C. Lee, H. Chen, and G. Fitzgerald, *J. Chem. Phys.* **102**, 1266 (1995).
- ⁶⁷D. A. Estrin, L. Paglieri, G. Corongiu, and E. Clementi, *J. Phys. Chem.* **100**, 8701 (1996).
- ⁶⁸S. S. Xantheas, *J. Chem. Phys.* **100**, 7523 (1994).
- ⁶⁹F. H. Stillinger and T. A. Weber, *Phys. Rev. A* **28**, 2408 (1983).
- ⁷⁰J. G. Nourse, *J. Am. Chem. Soc.* **102**, 4883 (1980).
- ⁷¹R. G. A. Bone, T. W. Rowlands, N. C. Handy, and A. J. Stone, *Mol. Phys.* **72**, 33 (1991).
- ⁷²H. C. Longuet-Higgins, *Mol. Phys.* **6**, 445 (1963).
- ⁷³P. R. Bunker, *Molecular Symmetry and Spectroscopy* (Academic, New York, 1979).
- ⁷⁴D. J. Wales, *J. Am. Chem. Soc.* **115**, 11191 (1993).
- ⁷⁵B. J. Dalton and P. D. Nicholson, *Int. J. Quantum Chem.* **9**, 325 (1975).
- ⁷⁶J. K. G. Watson, *Can. J. Phys.* **43**, 1996 (1965).
- ⁷⁷G. G. Hall, *Mol. Phys.* **83**, 551 (1977).
- ⁷⁸C. A. Coulson and S. Rushbrooke, *Proc. Camb. Phil. Soc.* **36**, 193 (1940).
- ⁷⁹D. Sabo, Z. Bačić, S. Graf, and S. Leutwyler, *Chem. Phys. Lett.* **261**, 318 (1996).